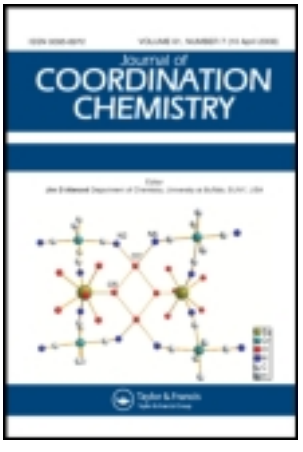

Journal of Coordination Chemistry
Publication details, including instructions for authors and subscription information:
http://www.tandfonline.com/loi/gcoo20

Supramolecular structures of metal complexes containing barbiturate and 1,2-bis(4-pyridyl)-ethane

Humberto C. Garcia [a], Filipe B. De Almeida [a], Renata Diniz [a], Maria I. Yoshida [b] & Luiz Fernando C. De Oliveira [a]

[a] Núcleo de Espectroscopia e Estrutura Molecular, Departamento de Química, Universidade Federal de Juiz de Fora, Campus Universitário s/n, Martelos, Juiz de Fora, MG 36036-900, Brazil

[b] Departamento de Química, Universidade Federal de Minas Gerais, Belo Horizonte, MG, Brazil

Published online: 04 Apr 2011.

To cite this article: Humberto C. Garcia, Filipe B. De Almeida, Renata Diniz, Maria I. Yoshida & Luiz Fernando C. De Oliveira (2011) Supramolecular structures of metal complexes containing barbiturate and 1,2-bis(4-pyridyl)-ethane, Journal of Coordination Chemistry, 64:7, 1125-1138

To link to this article: http://dx.doi.org/10.1080/00958972.2011.562894

Journal of Coordination Chemistry
Vol. 64, No. 7, 10 April 2011, 1125–1138

Supramolecular structures of metal complexes containing barbiturate and 1,2-bis(4-pyridyl)-ethane

HUMBERTO C. GARCIA†, FILIPE B. DE ALMEIDA†, RENATA DINIZ†, MARIA I. YOSHIDA‡ and LUIZ FERNANDO C. DE OLIVEIRA*†

†Núcleo de Espectroscopia e Estrutura Molecular, Departamento de Química, Universidade Federal de Juiz de Fora, Campus Universitário s/n, Martelos, Juiz de Fora, MG 36036-900, Brazil
‡Departamento de Química, Universidade Federal de Minas Gerais, Belo Horizonte, MG, Brazil

(*Received 4 November 2010; in final form 10 January 2011*)

This work describes the synthesis, thermal, spectroscopic properties (Raman and infrared), and crystal structures of five new supramolecular compounds $[Mn(bpa)(H_2O)_4]B_2 \cdot 4H_2O$ (**1**), $[Fe(bpa)(H_2O)_4]B_2 \cdot 4H_2O$ (**2**), $[Co(bpa)(H_2O)_4]B_2 \cdot 4H_2O$ (**3**), $[Zn(bpa)(H_2O)_4]B_2 \cdot 4H_2O$ (**4**), and $Co_2mal_2bpa \cdot 2H_2O$ (**5**), where B is the anion of barbituric acid, bpa is 1,2-bis(4-pyridyl)-ethane, and mal is malonate ion. Compounds **1**–**4** are isostructural, showing covalent linear 1-D $[M(bpa)(H_2O)_4]^{2+}$ chains, which interact by hydrogen-bonding and π-stacking interactions with barbiturate and crystallization water molecules resulting in a 3-D arrangement, belonging to *Pbcn* space group. Compound **5** has been obtained from the opening of the barbituric acid ring, with the formation of malonate, coordinated simultaneously to three cobalts in a 1-D chain along the *c*-axis, whereas bpa ligand gives rise to another 1-D chain along the *a*- and *b*-axes, resulting in a 3-D coordination polymer containing cavities. The vibrational spectra of **1**–**4** are also very similar; Raman spectra display two intense bands related to bpa at 1616 and 1020 cm^{-1}, assigned to the (ν_{CC}/ν_{CN}) and ring stretching modes, respectively. The barbiturate is also confirmed by a band at 684 cm^{-1}; the interesting point to be emphasized is this vibrational mode is not observed for **5**, corroborating the absence of this building block in the structure.

Keywords: Supramolecular structures; Metal complexes; Raman spectroscopy; Barbituric acid; Malonate ion

1. Introduction

Synthesis of metallic–organic complexes has attracted interest from a structural point of view and due to their potential applications in catalysis, electrical conductivity, magnetism, and photochemistry [1–5]. There is growing interest on the design and construction of metallic–organic polymers achieving supramolecular structures based on strong covalent metal–ligand interactions as well as weak intermolecular forces, such as hydrogen bonding, Coulombic, and π-stacking interactions [6–8]. These weak non-covalent interactions, especially hydrogen bonds, play a crucial role in fundamental

*Corresponding author. Email: luiz.oliveira@ufjf.edu.br

ISSN 0095-8972 print/ISSN 1029-0389 online
DOI: 10.1080/00958972.2011.562894

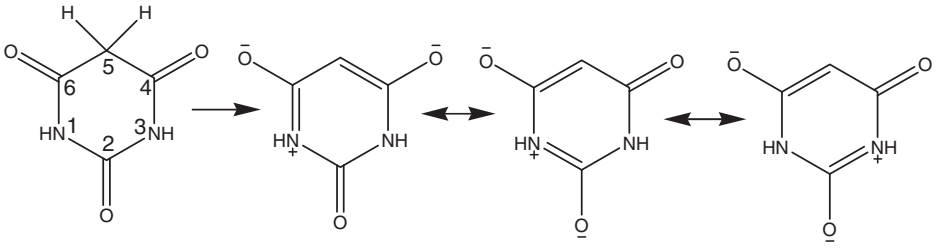

Figure 1. Molecular structure of barbituric acid, barbiturate, and the resonance forms (adapted from reference [14]).

biological processes, such as the expression and transfer of genetic information. These forces are also essential for molecular recognition between receptors and substrates, as well as for the construction of complicated supramolecular arrays [9, 10].

Barbiturates and derivatives are building blocks recently employed in constructing crystalline arrays for properties as molecular memory storage, non-linear optical materials (NLO), and strong fluorescent properties [11–13]. Barbiturates belong to a group of drugs derived from barbituric acid (figure 1) [14], acting as depressants of the central nervous system and presenting powerful sedative and hypnotic properties [14, 15]. The presence of several potential donors such as two amine nitrogens and three carbonyl oxygens makes barbiturates very interesting polyfunctional ligands in coordination chemistry [16, 17].

Another well-known ligand in supramolecular chemistry is 1,2-bis(4-pyridyl)-ethane (bpa), which has been extensively employed as organic building block for construction of 1-D, 2-D and 3-D networks. It can be used in coordination chemistry as a bidentate bridging ligand [18], but can also act as a terminal ligand [19] or as a host molecule [20]. Bpa can exhibit different conformation geometries, due to the presence of the flexible ethyl group between the pyridine rings, which may be further involved in hydrogen-bonding and/or π-stacking interactions [21]. Another important feature is related to the properties of new materials containing bpa, ranging from magnetism and catalysis to NLO [22, 23].

This work describes the conventional synthesis, spectroscopic, and structural characterization of four new coordination complexes obtained from the building blocks 1,2-bis(4-pyridyl)-ethane (bpa) and barbiturate with Mn^{2+}, Fe^{2+}, Co^{2+}, and Zn^{2+}. The solvothermal synthesis has also been used for the supramolecular system involving bpa, barbiturate, and Co^{2+}, which has been characterized by X-ray diffraction and vibrational spectroscopy. This is the first work describing the opening ring of the barbituric acid structure giving rise to malonate, from the use of solvothermal synthesis.

2. Experimental

2.1. *Chemicals and reagents*

All chemicals and solvents were used as purchased: $MnSO_4 \cdot H_2O$ (98.0%, Vetec), $FeSO_4 \cdot 7H_2O$ (99.5%, Sigma Aldrich), $CoCl_2 \cdot 6H_2O$ (99.5%, Sigma Aldrich),

$ZnSO_4 \cdot 7H_2O$ (99.0%, Vetec), barbituric acid ($C_4H_4N_2O_3$, 99.0%, Merck), and 1,2-bis(4-pyridyl)-ethane (98.0%, Sigma Aldrich).

2.2. *Synthesis*

Generally, the synthesis method is the same for all compounds: 10.0 mL of an aqueous solution containing 34.0 mg (0.27 mmol) of barbituric acid (HB) were added to 10.0 mL of an ethanolic solution containing 50.0 mg (0.27 mmol) of 1,2-bis(4-pyridyl)-ethane (bpa), resulting in a homogeneous colorless solution; to this solution was added the solution with the metallic ion, according to the following description. For complexes of general formula $Mn(bpa)(H_2O)_4]B_2 \cdot 4H_2O$ (**1**), $[Fe(bpa)(H_2O)_4]B_2 \cdot 4H_2O$ (**2**), $[Co(bpa)(H_2O)_4]B_2 \cdot 4H_2O$ (**3**), and $[Zn(bpa)(H_2O)_4]B_2 \cdot 4H_2O$ (**4**), it was added slowly by diffusion of 5.0 mL of an aqueous solution containing 0.27 mmol of $MnSO_4 \cdot H_2O$, $FeSO_4 \cdot 7H_2O$, $CoCl_2 \cdot 6H_2O$, or $ZnSO_4 \cdot 7H_2O$. After a few days suitable single crystals were obtained, being colorless for **1** (yield = 35%) and **4** (yield = 40%), yellow for **2** (yield = 33%), and orange for **3** (yield = 40%). For the synthesis of $Co_2mal_2bpa \cdot 2H_2O$ (**5**), 5.0 mL of an aqueous solution containing $CoCl_2 \cdot 6H_2O$ was added, followed by 5 min of stirring, generating an orange solution, which was transferred and sealed in a 30 mL Teflon-lined autoclave, being subjected to solvothermal conditions at 120°C for 40 h, and cooled to room temperature at $5°C\,h^{-1}$. After opening the reaction vessel pink crystals (yield = 10%) suitable for X-ray diffraction were observed. Elemental analysis: $[Mn(bpa)(H_2O)_4]B_2 \cdot 4H_2O$ (**1**): Calcd (%): C, 37.68; H, 5.38; N, 13.18. Found (%): C, 37.86; H, 5.72; N, 12.71. $[Fe(bpa)(H_2O)_4]B_2 \cdot 4H_2O$ (**2**): Calcd (%): C, 37.63; H, 5.37; N, 13.17. Found (%): C, 37.72; H, 5.53; N, 12.98. $[Co(bpa)(H_2O)_4]B_2 \cdot 4H_2O$ (**3**): Calcd (%): C, 37.45; H, 5.34; N, 13.10. Found (%): C, 37.56; H, 4.89; N, 12.66. $[Zn(bpa)(H_2O)_4]B_2 \cdot 4H_2O$ (**4**): Calcd (%): C, 37.08; H, 5.29; N, 12.97. Found (%): C, 37.35; H, 5.15; N, 12.95 and $Co_2mal_2bpa \cdot 2H_2O$ (**5**): Calcd (%): C, 39.87; H, 3.72; N, 5.17. Found (%): C, 39.74; H, 3.81; N, 5.13.

2.3. *Physical measurements*

Thermogravimetric (TG/DTA) measurements were done using a Shimadzu TG-60 with thermo balance; samples were heated at $10°C\,min^{-1}$ from room temperature to 750°C in dynamic nitrogen with a flow rate equal to $100\,mL\,min^{-1}$. Infrared (IR) spectra were obtained using a Bomem MB-102 spectrometer fitted with a CsI beam splitter, with the samples dispersed in KBr pellets and a spectral resolution of $4\,cm^{-1}$; good signal-to-noise ratios were obtained from accumulation of 128 spectral scans. Fourier-transform Raman spectroscopy was carried out using a Bruker RFS 100 instrument, Nd^{3+}/YAG laser operating at 1064 nm in the near-IR and CCD detector cooled with liquid N_2; good signal-to-noise ratios were obtained from 1000 scans accumulated over a period of about 30 min using $4\,cm^{-1}$ as spectral resolution. All spectra were obtained at least twice to show reproducibility, and no changes in band positions and intensities were observed. Single crystal X-ray data were collected using an Oxford GEMINI A Ultra diffractometer with Mo-Kα ($\lambda = 0.71073$ Å) at room temperature (298 K). Data collection, reduction, and cell refinement were performed by CrysAlis RED, Oxford Diffraction Ltd – Version 1.171.32.38 program [24]. The structures were solved and refined using SHELXL-97 [25]. An empirical isotropic extinction parameter x was

refined according to the method described by Larson [26]. A Multiscan absorption correction was applied [27]. The structures were drawn by ORTEP-3 for windows [28] and Mercury [29] programs.

3. Results and discussion

To study the stability of the coordination polymers, TG measurements were performed under nitrogen; the TG curves of **1**–**4** are deposited as Supplementary materials (figures S1–S4). All curves exhibit very similar profile, with two consecutive mass losses at *ca* 100°C, related to the loss of all water molecules present in the structure (both crystallization and coordination water molecules). Other successive mass losses are observed for all complexes with temperature increasing from *ca* 180°C, referring to the thermodecomposition of the compounds, and ending with a residue related to the metal oxide at 750–850°C.

The structures of **1**, **2**, **3**, and **5** have been revealed by X-ray single crystal analysis. Compound **4** did not produce suitable single crystals for X-ray diffraction analysis; nevertheless, the unit cell of this complex could be obtained ($a = 10.2677(1)$ Å, $b = 14.5372(1)$ Å, $c = 18.8234(2)$ Å) and is almost the same for **1**, **2**, and **3** (table 1), strongly suggesting that the Zn(II) compound is isomorphous to the Fe(II), Mn(II), and Co(II) complexes.

Figure 2 shows the molecular 1-D arrangement of **1**–**3**, displaying the cationic unit composed by metal coordinated in a slightly distorted octahedral geometry, from four water molecules in the equatorial positions and two pyridyl nitrogens from two different bpa ligands in the axial positions. The entire structure for the three compounds is neutralized by two uncoordinated barbiturate anions, belonging to the orthorhombic *Pbcn* space group. The averages of M–O and M–N bond distances are 2.168(2) and 2.281(2) Å for **1**, 2.098(2) and 2.229(1) Å for **2**, and 2.085(3) and 2.176(3) Å for **3**. In all compounds M–N is longer than M–O. The longest M–N distance is observed for **3**, explained by the difference in ionic radius of the metallic sites, which decrease with the increasing atomic number from Fe(II) to Co(II). Distances between two adjacent metallic sites connected by bpa in a bis-monodentate mode are 13.929, 13.878, and 13.762 Å for **1**, **2**, and **3**, respectively. Other important bond distances for the complexes, together with their angles, are shown in table 2.

The 3-D arrangement *via* covalent bonds and hydrogen-bond interactions for **1**–**3** are displayed in figure 3; observation along the *ac* diagonal plane reveals the presence of layers, formed by $[M(bpa)(H_2O)_4]^{2+}$ 1-D parallel linear chains. Another layer can also be observed through hydrogen interaction between barbiturate and water. The supramolecular interaction between barbiturates can be classified as moderate to weak, according to the geometric parameters [30–33]. The NH of one barbiturate is a hydrogen donor and interacts with the carbonyl of another barbiturate, O···N (O5···N3) at distances of 2.855(2), 2.786(2), and 2.825(4) Å for **1**, **2**, and **3**, respectively. Interaction between two consecutive layers occurs through hydrogen bonds, promoted by the two types of water (crystallization and coordination) and barbiturate. All hydrogen interactions which can be observed for **1**–**3**, with distances of interaction, can be seen in table 3 for comparison. An interesting aspect for supramolecular structure analysis comes from the centroid–centroid distances; for **1**, **2**, and **3** the distances

Table 1. Crystal data of $[M(bpa)(H_2O)_4]B_2 \cdot 4H_2O$ (where $M = Mn^{2+}$, Fe^{2+}, and Co^{2+}) and $Co_2mal_2bpa \cdot 2H_2O$ (**5**).

Compound	$[Mn(bpa)(H_2O)_4]B_2 \cdot 4H_2O$ (**1**)	$[Fe(bpa)(H_2O)_4]B_2 \cdot 4H_2O$ (**2**)	$[Co(bpa)(H_2O)_4]B_2 \cdot 4H_2O$ (**3**)	$Co_2mal_2bpa \cdot 2H_2O$ (**5**)
Empirical formula	$C_{20}H_{34}MnN_6O_{14}$	$C_{20}H_{34}FeN_6O_{14}$	$C_{20}H_{34}CoN_6O_{14}$	$C_{18}H_{20}Co_2N_2O_{10}$
Formula weight ($g\,mol^{-1}$)	637.47	638.38	625.46	542.22
Crystal system	Orthorhombic	Orthorhombic	Orthorhombic	Orthorhombic
Space group	*Pbcn*	*Pbcn*	*Pbcn*	*Pnnm*
Unit cell dimensions (Å, °)				
a	10.268	10.230	10.182	20.778(4)
b	14.537	14.319	14.400	6.884(14)
c	18.823	18.755	18.517	7.504(15)
Volume $(Å)^3$, *Z*	2809.6, 4	2747.2, 4	2715.0, 4	1073.3(4), 2
Calculated density ($g\,cm^{-3}$)				
Absorption coefficient, μ(Mo-Kα) (cm^{-1})	0.547	0.628	0.707	1.603
Crystal size (mm^3)	$0.12 \times 0.26 \times 0.42$	$0.14 \times 0.38 \times 0.46$	$0.07 \times 0.12 \times 0.40$	$0.16 \times 0.33 \times 0.51$
	1.507	1.543	1.530	1.678
Reflections collected	27,018	9101	24,670	9182
Independent reflection	3703	3352	3613	1193
Observed reflections $[F_0^2 > 2\sigma(F_0^2)]$	2098	2401	1330	1087
Max. and min. transmission	0.8932/1.000	0.7971/1.000	0.9428/1.000	0.8081/1.000
No. of parameters refined	197	214	202	97
R $[F_0 > 2\sigma(F_0)]$	0.0497	0.0360	0.0572	0.0211
wR $[F_0^2 > 2\sigma(F_0)^2]$	0.1684	0.0915	0.1425	0.0565
S	1.012	1.067	0.789	1.12
Largest difference peak and hole ($e\,Å^{-3}$)	0.074	0.068	0.097	0.049

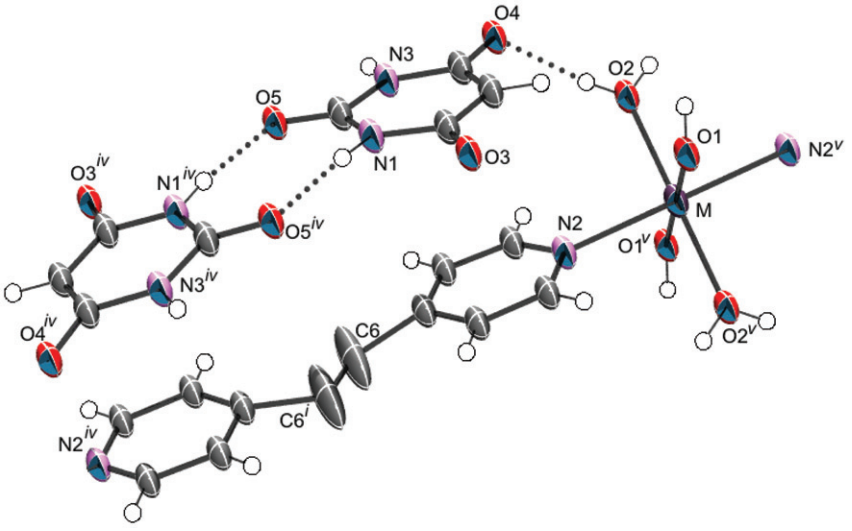

Figure 2. ORTEP representation of the 1-D covalently bonded chain and barbiturate. Thermal ellipsoids are drawn at the 50% probability level for **1**–**3**. Water molecules are omitted for clarity. Symmetry code: [i]: x, y, z; [iv]: $-x$, y, $-z+\frac{1}{2}$; [v]: $-x$, $-y$, $-z$.

between the barbiturate rings and pyridyl rings (figure 3) are 3.67(1), 3.60(1), and 3.63(2) Å, respectively, indicating the existence of π-stacking interactions between bpa and barbiturate arising from different layers along the *b*-axis and contributing to the crystal lattice stability. Garcia *et al.* [34] synthesized similar systems consisting of $[M(bpy)(H_2O)_4]^{2+}$ (bpy is 4,4′-bipyridine) with covalent chains neutralized by barbiturate anions, but the presence of the π-stacking interaction was not verified. For the compounds investigated here the π-stacking interaction can be explained due to the accommodation of the barbiturate charge density over the $[M(bpa)(H_2O)_4]^{2+}$ covalent chain, being favored by geometrical parameters such as the presence of the ethyl group ($-CH_2-CH_2-$), which is responsible for increasing the distance between the pyridyl rings of the chains. Comparing both structures, the π-stacking interactions observed for **1**–**3** show up mainly due to the lack of two crystallization water molecules, which are present in the previous supramolecular arrangement described by Garcia *et al.* [34]. In recent investigations involving coordination of other types of barbituric acid analogs, Aksoy *et al.* [35] and Yilmaz *et al.* [36] have coordinated 5,5-diethylbarbiturato to copper and nickel metal sites through nitrogens and oxygens. The success of that coordination strategy may be due to the lack of the acid hydrogen on C5 (for numbering see figure 1) in the 5,5-diethylbarbiturato structure, which is bonded to two ethyl groups, thus enabling coordination by NH of the structure. However, despite the little information about supramolecular interactions in these particular works, it can be seen that the main driving forces over the solid structure are the hydrogen bonds [35, 36].

Figure 4 displays the repeating unit of $Co_2mal_2bpa \cdot 2H_2O$ (**5**) as a coordination polymer composed of two metallic sites featuring a slightly distorted octahedral geometry. The bpa coordinates in the bridge mode between two metal centers and each metal is also coordinated to a single water molecule and two malonates. Malonate was not an added reactant, being produced during the reaction; for this specific synthesis

Table 2. Selected geometrical parameters of $[M(bpa)(H_2O)_4]B_2 \cdot 4H_2O$ and $Co_2mal_2bpa \cdot 2H_2O$ (**5**) taking into account the hydrogen-bonding interaction.

	$[Mn(bpa)(H_2O)_4]B_2 \cdot 4H_2O$ (**1**)	$[Fe(bpa)(H_2O)_4]B_2 \cdot 4H_2O$ (**2**)	$[Co(bpa)(H_2O)_4]B_2 \cdot 4H_2O$ (**3**)		$Co_2mal_2bpa \cdot 2H_2O$ (**5**)
Bond distance (Å)					
M–N2	2.281(2)	2.229(1)	2.176(3)	M–N2	2.146(2)
M–O1	2.174(2)	2.097(1)	2.096(3)	M–O1	2.135(2)
M–O2	2.163(2)	2.100(1)	2.075(3)	M–O3	2.086(9)
N2–C5	1.324(4)	1.340(2)	1.334(4)	M–O4	2.109(9)
N2–C1	1.328(4)	1.339(2)	1.333(4)	O4–C11	1.248(2)
O4–C8	1.271(3)	1.242(2)	1.273(4)	O3–C11	1.264(2)
N3–C9	1.352(3)	1.356(2)	1.335(5)	N2–C1	1.332(2)
N3–C7	1.393(3)	1.392(2)	1.381(4)	C11–C12	1.523(2)
C9–O5	1.230(3)	1.242(2)	1.237(4)	C3–C2	1.378(2)
C9–N1	1.362(3)	1.356(2)	1.361(5)	C3–C6	1.507(3)
C10–C8	1.381(3)	1.386(2)	1.383(5)	C1–C2	1.388(2)
C10–C7	1.384(3)	1.392(2)	1.365(5)	C6–C6	1.509(5)
N1–C8	1.387(3)	1.388(2)	1.379(4)	–	–
O3–C7	1.258(3)	1.266(2)	1.284(4)	–	–
Average of bond angles (°)					
O–M–O	180.0	180.0	180.0	–	172.40(3)
O–M–O	90.49(9)	90.01(6)	90.65(11)	O–M–O	86.42(4)
N–M–O	93.67(7)	94.20(5)	93.64(11)	N–M–O	91.04(4)
N–M–N	180.0	180.0	180.0	N–M–N	178.16(6)
D···A (Å)	–	–	–	–	–
O2···O7	2.636(4)	2.679(2)	2.710(4)	–	–
O1···O3	2.795(3)	2.758(2)	2.732(4)	–	–
N1···O4	2.810(2)	2.841(2)	2.788(4)	–	–
O2···O5	2.748(3)	2.753(2)	2.791(4)	–	–
O6···O5	2.900(3)	2.878(2)	2.834(9)	–	–
N3···O5	2.855(3)	2.786(2)	2.825(4)	D···A (Å)	–
O7···O3	2.893(4)	2.818(2)	2899(4)	O1···O3	2.650(1)
O6···O3	2.813(3)	2.813(3)	2.843(9)	–	–
O7···O5	2.804(4)	2.804(4)	2.813(4)	–	–
D–H···A (°)	–	–	–	D–H···A (°)	–
O1–H1A···O3	142	170(2)	–	O1–H1A···O3	160(2)
N1–H1N···O4	176	174	–	–	–
O2–H2B···O5	169	175	–	–	–
O7–H7B···O3	139	157		–	–

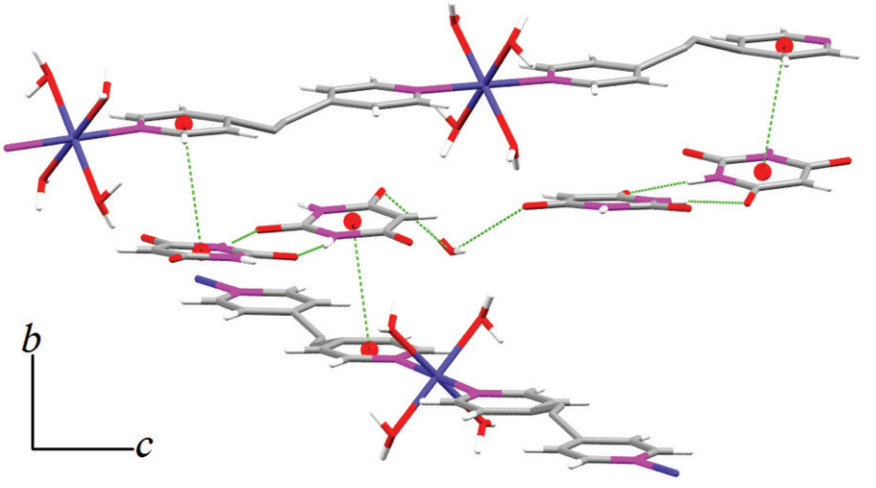

Figure 3. Layers formed by covalent bonds for $[M(bpa)(H_2O)_4]^{2+}$ and supramolecular interactions of hydrogen bonding and π-stacking interactions, generating a 3-D arrangement of the complexes.

under high pressure and temperature conditions, figure S5 (Supplementary material) displays a tentative scheme to understand the production of malonate from barbituric acid. The acidic environment provided by the barbituric acid deprotonation probably promotes attack on the carbonyl oxygen by H^+, followed by attack on the carbonyl carbon by water, leading to ring opening and formation of malonic acid and urea, the same products which are involved in the synthesis of barbituric acid [37]. Figure 5 shows the 3-D arrangement of the structure containing only covalent bonds, formed by bidentate malonate monodentate to two metal centers along the *c*-axis (figure 5a); along the *a*-axis bpa is a bridge between two metal sites, generating a kind of ladder that extends indefinitely. A rectangular cavity generated by four metal ions, two bpa, and two malonate ligands is formed with a volume of *ca* 356 Å^3 (this volume has been calculated by using the rectangle volume approximation). Due to this cavity and the lack of crystallization water in the structure, this complex could act as a gas absorber in complex systems. Figure 5(b) shows the existence of the chain zigzag along the *ab* plane, with the presence of water in the terminal position of the chain connected to the metal center which serves as a connector to an adjacent chain. The angle between the molecular planes of this zigzag design is about 88°. The existence of supramolecular interactions is evidenced by the presence of π-stacking interactions between two pyridyl rings of adjacent bpa as in figure 5b, with centroid–centroid distance of 3.84(2) Å. Another supramolecular interaction is observed through a single hydrogen bond that occurs between $O3\cdots O1 = 2.650(1)$ Å. These interactions together with the new covalent bonds formed are responsible for crystal stability of the entire complex. The description of this polymer has been made by the TOPOS program package [38], where the metal site (Co^{2+}) is considered as the node; this coordination polymer is constituted by a 7-connected uninodal net that can be described with short Schläfli symbols $3^6 4^8 5^7$. Figure 6 displays a fragment of the net formed in **5**, where it is possible to see all seven connections (figure 6a) as well as some circuits generated from the Co^{2+} node (figure 6b). In this last figure it is also possible to note the presence of the three distinct circuits described by short Schläfli nomenclature: the three-membered circuit formed by

Table 3. Raman and IR wavenumbers (in cm^{-1}) and tentative assignment of the most important bands in $[M(bpa)(H_2O)_4]B_2 \cdot 4H_2O$ and $Co_2mal_2bpa \cdot 2H_2O$.

Barbiturate anion		bpa		Mn (**1**)		Fe (**2**)		Co (**3**)		Zn (**4**)		$Co_2mal_2bpa\ 2H_2O$ (**5**)		Tentative assignment
IR	R	IR	R	IR	R	IR	R	IR	R	IR	R	IR	R	
–	–	–	–	544 m	537 m	546 m	540 m	544 m	539 m	542 m	539 m	–	–	ν_{M-N}
–	–	548 vs	–	–	–	–	–	–	–	–	–	–	–	$\delta_{o.p.\ CH} + \delta_{wagg\ CH2}$
–	620 w	–	–	–	–	–	–	–	–	–	–	–	–	$\delta_{o.p.\ CO}$
–	684 vs	–	–	–	684 vs	–	684 vs	–	686 vs	–	686 vs	–	–	Ring breathing
–	–	–	–	–	–	–	–	–	–	–	–	710 m	–	δ_{OCO} (Ma)
–	–	830 vs	–	831 m	–	831 m	–	835 m	–	835 m	–	–	–	$\delta_{o.p\ CH}$
–	–	–	873 m	–	877 w	–	878 w	–	–	–	–	–	886 w	$\delta_{o.p\ CH}$
–	969 m	–	–	–	988 m	–	990 m	–	988 m	–	989 m	–	–	ν_{ring}
–	–	991 m	995 vs	–	1016 vs	–	1014 vs	–	1018 vs	–	1018 vs	–	1025 vs	ν_{ring}
–	–	–	1216 s	1215 w	1216 m	1222 w	1213 m	1217 m	1216 m	1213 m	1214 m	–	1212 m	$\delta_{i.p\ CH}$
1234 m	–	–	–	–	1236 m	–	1234 m	–	1236 m	–	1236 m	–	–	ν_{CN}
1300 m	–	–	–	1298 s	–	1298 s	–	1294 s	–	1301 s	–	–	–	$\nu_{ring} + \delta_{o.p\ CH}$
–	–	–	–	–	–	–	–	–	–	–	–	1358 m	–	ν_{asCC} (Ma)
1369 w	1367 w	–	–	1360 s	–	1362 s	–	1362 s	–	1369 s	–	–	–	$\delta_{i.p.NH}$
1412 s	–	–	–	1398 m	–	1400 m	–	1396 m	–	1416 m	–	–	–	ν_{CN}
–	–	1414 s	–	–	–	–	–	–	–	–	–	–	–	$\nu_{ring} + \delta_{o.p\ CH}$
–	–	–	–	–	–	–	–	–	–	–	–	1576 vs	–	$\nu_{OCO(as)}$ (Ma)
–	–	1597 vs	1598 s	1614 vs	1615 s	1614 vs	1614 vs	1610 vs	1615 s	1618vs	1616 vs	1620 s	1619 s	ν_{CC}/ν_{CN}
1636 s	1627 w	–	–	–	–	–	–	–	–	–	–	–	–	$\nu_{C2=O}$
1688 vs	1702 w	–	–	1699 vs	–	1703 vs	–	1691 vs	–	1684 vs	–	–	–	$\nu_{C4,6=O}$
–	–	–	2924 s	–	2911 m	–	2908 m	–	2911 m	–	2911 m	–	2924 vs	ν_{CH2}
–	–	–	3054 vs	–	3070 s	–	3070 s	–	3073 vs	–	3075 s	–	3083 vs	ν_{CH}
–	3114 m	–	–	–	3111 m	–	3113 m	–	3108 m	–	3113 m	–	–	ν_{NH}

Abbreviations: R, Raman; IR, infrared; vs, very strong; s, strong; m, medium; w, weak; B, barbiturate anion; i.p., in-plane; o.p., out-of-plane; wag, wagging, scissor.

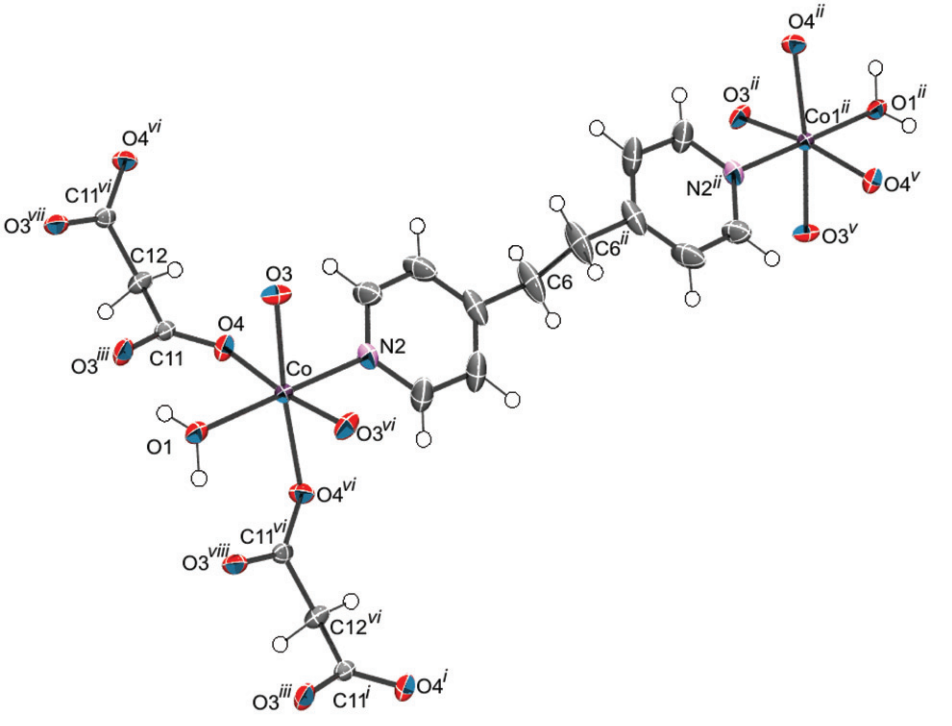

Figure 4. ORTEP representation of the 2-D covalently bonded chain. Thermal ellipsoids are drawn at the 50% probability level for **5**. Symmetry code: [i]: x, y, z; [ii]: $-x, -y, z$; [iii]: $-x+\frac{1}{2}, y+\frac{1}{2}, -z+\frac{1}{2}$; [v]: $-x, -y, -z$; [vi]: $x, y, -z$; [vii]: $x+\frac{1}{2}, -y+\frac{1}{2}, z+\frac{1}{2}$; [viii]: $-x+\frac{1}{2}, y+\frac{1}{2}, z+\frac{1}{2}$.

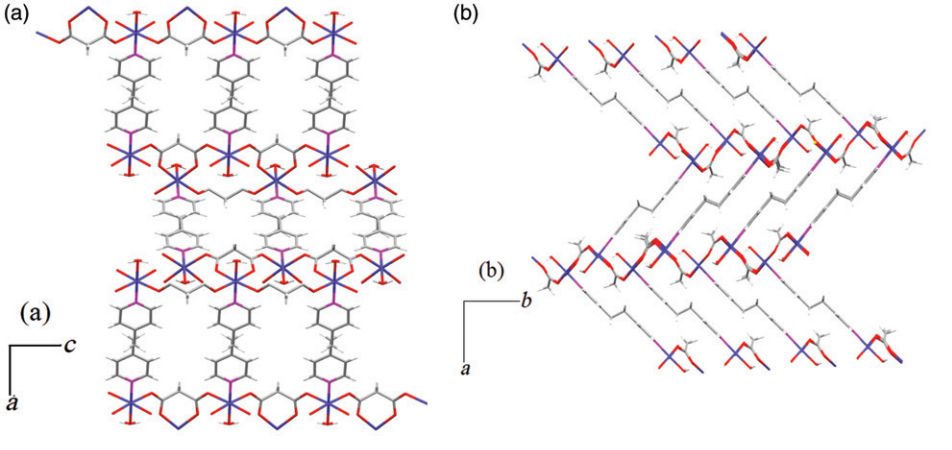

Figure 5. 3-D view of the structure of **5**: (a) in the form of stairs along the *ac* plane, (b) in the form of zigzag along the *ab* plane.

atoms labeled 1, 2, and 3; the four-membered formed by atoms 1, 4, 5, and 6, and the five-membered generated by 1, 2, 7, 8, and 3 atoms.

The vibrational spectra of all ligands and complexes investigated in this work are displayed in figure S6 and figure 7 (IR and Raman spectra, respectively). All spectra are

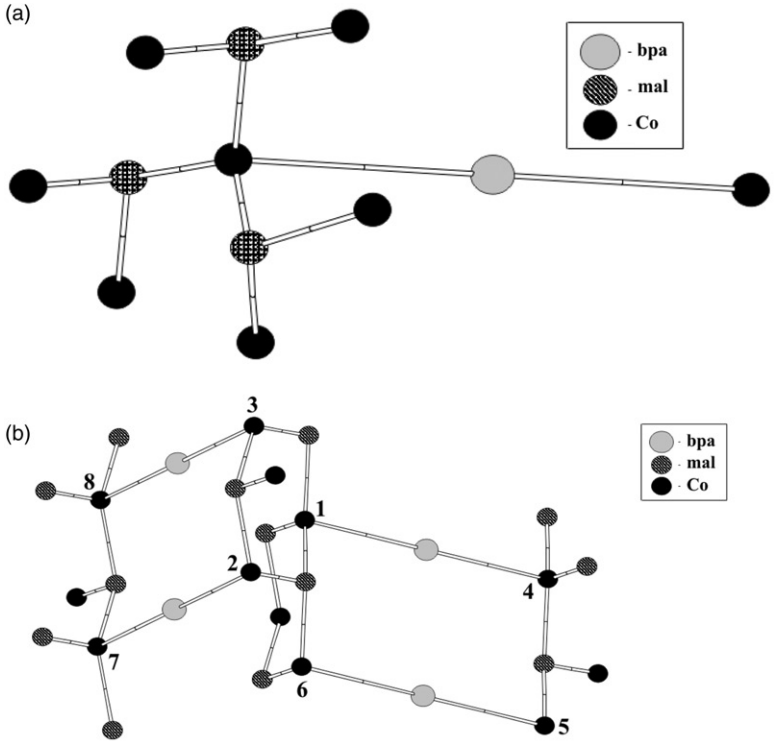

Figure 6. Schematic view of **5** obtained by TOPOS program showing (a) the 7-connections from Co1 and (b) some circuits formed by this polymer. The Co^{2+} is considered as the node of the net.

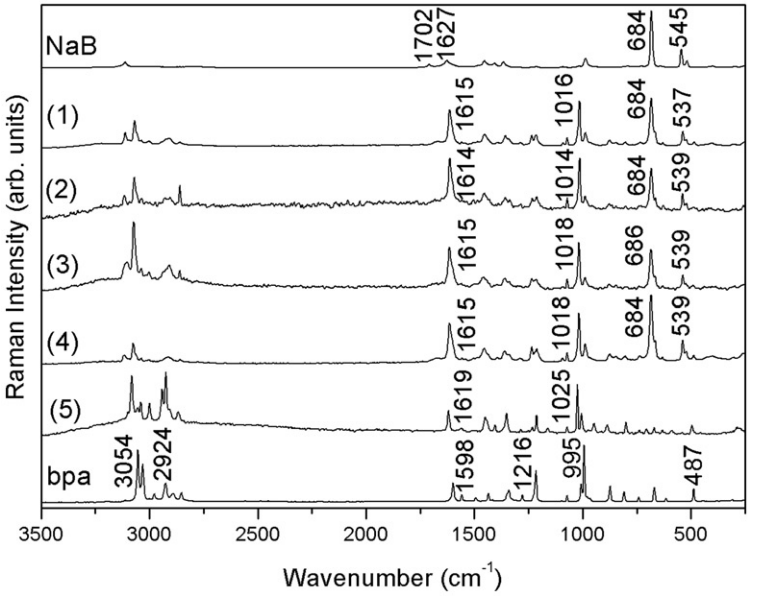

Figure 7. Raman spectra of **1–5**; for comparison spectra of bpa and B^- are also displayed.

very similar and are in agreement with the crystal data, indicating the same molecular arrangement for all compounds. The main vibrational bands are summarized in table 3 as well as the respective tentative vibrational assignments based on similar chemical systems [34, 39–41].

From the analysis of the barbiturate IR spectrum, a very broad band in the 3300–3600 cm^{-1} region can be observed, assigned to stretching modes of H_2O and NH; this band is also observed for all coordination complexes, except for **5**. Two intense bands at 1688 and 1636 cm^{-1} can be assigned to $\nu_{C=O}$ of the carboxyl group (referring to $C_{4,6}$ and C_2, respectively). This band appears shifted by *ca* 40 and 60 cm^{-1} to lower wavenumbers when compared to free barbituric acid, being observed at 1730 and 1694 cm^{-1} [42]. This may be explained by the loss of the acidic hydrogen and a consequent increase of electronic delocalization over the carboxyl groups, with the formation of the resonance structure represented in figure 1. In the Raman spectrum of the barbiturate anion a single and very intense band at 684 cm^{-1} can be observed, assigned to the ring breathing mode. This same vibrational mode appears originally in barbituric acid as a band at 665 cm^{-1}, shifting to higher wavenumbers due to the electronic delocalization through the ring due to the formation of the barbiturate anion (figure 1). Therefore, this mode is very important for the confirmation of the presence of barbiturate anion in the complexes. Bands of less intensity can be seen at 1627 and 1702 cm^{-1}, assigned to ν_{CO}.

In the IR spectrum of free 1,2-bis(4-pyridyl)-ethane, an intense band at 1597 cm^{-1} can be observed, tentatively assigned to the coupled (ν_{CC}/ν_{CN}) stretching modes of the pyridyl rings. Bands at 1414 and 830 cm^{-1} are attributed to ($\nu_{ring} + \delta_{CH}$) and δ_{CH}, respectively. In the Raman spectrum the most intense and characteristic bands are at 1216 cm^{-1}, assigned to δ_{CH}, and at 1598 and 995 cm^{-1}, assigned to the (ν_{CC}/ν_{CN}) stretching and ν_{ring}, respectively. Experimental observations have been made where bands at 1597 (IR) and 1598 cm^{-1} (Raman) for the free ligand shift to higher wavenumbers when the ligand is coordinated to metal [37, 43].

For **1**–**4** IR spectra exhibit intense bands characteristic of barbiturate (B^-) around 1690 cm^{-1}, assigned to the CO stretching mode [ν_{CO}]. Other bands at *ca* 1300, 1360, and 1400 cm^{-1} can be related to $\nu_{ring} + \delta_{CH}$, δ_{NH}, and ν_{CN} modes, respectively. These last three bands have the same profile for all the coordination compound's spectra, indicative of the presence of barbiturate in the supramolecular arrangement. For **5**, bands for barbiturate are not observed, confirming its absence. Bands at 710, 1358, and 1576 cm^{-1} can be tentatively assigned to δ_{OCO}, ν_{CC}, and ν_{OCO} of malonate, respectively. The presence of bpa in the IR spectrum of each compound is confirmed by characteristic band at *ca* 830 cm^{-1}, assigned to δ_{CH}, and at 1615 cm^{-1}, attributed to (ν_{CC}/ν_{CN}) of pyridyl ring. This last mode appears shifted to higher wavenumbers when compared to the free ligand spectrum (appearing at 1597 cm^{-1}), confirming coordination of the ligand to the metal center.

Raman spectra of all the synthesized compounds display characteristic bands at 1615 and 1020 cm^{-1}, assigned to (ν_{CC}/ν_{CN}) and ring stretching modes (ν_{ring}) of bpa. Another characteristic, but not intense, band for this ligand can be observed at 1215 cm^{-1}, assigned to (δ_{CH}). The presence of the barbiturate in **1**–**4** can be confirmed by an intense band at 684 cm^{-1}, assigned to ring breathing (ν_{ring}); this band can also be understood as a specific marker for the presence of the barbiturate. For **5** this band is not observed,

showing the advantage of using spectroscopic techniques, such as IR and Raman, for the study of these supramolecular systems.

As a final remark, the metallic centers Mn(II), Fe(II), Co(II), and Zn(II) investigated in this work seem to be less important for generating the supramolecular structure than the ligands, since all the complexes appear isostructural, with almost the same hydrogen bonds and π-stacking interactions. For Co(II), another structure was produced, originated by cleaving the barbiturate ring, giving malonate. However, the obtained supramolecular structure appears to be similar to the others when the solid-state forces are compared; similar hydrogen bonds are responsible for the 3-D arrangement.

4. Conclusions

Synthesis of five supramolecular complexes $[Mn(bpa)(H_2O)_4]B_2 \cdot 4H_2O$, $[Fe(bpa)(H_2O)_4]B_2 \cdot 4H_2O$, $[Co(bpa)(H_2O)_4]B_2 \cdot 4H_2O$, $[Zn(bpa)(H_2O)_4]B_2 \cdot 4H_2O$, and $Co_2mal_2bpa \cdot 2H_2O$ are reported. For **1**, **2**, and **4** the formation of a covalent linear 1-D chain $[M(bpa)(H_2O)_4]^{2+}$ has been observed, interacting by hydrogen bonds and π-stacking interactions with barbiturate and crystallization and coordination water molecules, resulting in a 3-D arrangement. For **5** opening of the barbiturate ring with the formation of malonate, unprecedented in the literature of barbituric acid coordination chemistry, has been observed. The 3-D coordination polymer formed presents a short Schläfli symbol $3^6 4^8 5^7$. In the IR spectra for **1**–**4** a band at *ca* 1690 cm^{-1} is observed for ν_{CO} of barbiturate. For **5** this band is not seen, suggesting the absence of barbiturate in the supramolecular structure. The Raman spectra confirm these observations. This work demonstrates that multifunctional organic ligands containing nitrogens and carbonyl groups (with H-donors and H-acceptors), together with specific solvent, and synthetic methodology (diffusion or solvothermal) have the potential to give different compounds.

Supplementary material

CCDC numbers 787745, 787743, 787742, and 787744 contain the supplementary crystallographic data for **1**, **2**, **3**, and **5**, respectively; these data can be obtained free of charge at http://www.ccdc.cam.ac.uk or from the Cambridge Crystallographic Data Centre, 12 Union Road, Cambridge CB2 IEZ, UK (Fax: (Internat.) 1 44-1223/336-033; E-mail: deposit@ccdc.cam.ac.uk).

Acknowledgments

The authors thank CNPq, CAPES, FAPEMIG (PRONEX 526/07, CEX-APQ-00617/09), and FINEP (PROINFRA 1124/06) for the financial support and also LabCri (Departamento de Física – Universidade Federal de Minas Gerais) for the X-ray facilities.

References

[1] L. Wang, Q. Chen, G.-B. Pan, L.-J. Wan, S. Zhang, X. Zhan, B.H. Northrop, P.J. Stang. *J. Am. Chem. Soc*., **130**, 13433 (2008).
[2] R.L. Laduca. *Coord. Chem. Rev*., **253**, 1759 (2009).
[3] M. Fujita, Y.J. Kwon, S. Washizu, K. Ogura. *J. Am. Chem. Soc*., **116**, 1151 (1994).
[4] S. Marivel, M.R. Shimpi, V.R. Pedireddi. *Cryst. Growth Des*., **7**, 1791 (2007).
[5] L. Soto, J. Garcia, E. Escriva, J.P. Legros, J.P. Tuchagues, F. Dahan, A. Fuertes. *Inorg. Chem*., **28**, 3378 (1989).
[6] A.N. Khlobystov, A.J. Blake, N.R. Champness, D.A. Lemenovskii, A.G. Majouga, N.V. Zyk, M. Schröder. *Coord. Chem. Rev*., **222**, 155 (2001).
[7] G.S. Nichol, W. Clegg. *Cryst. Growth Des*., **9**, 1844 (2009).
[8] M. Ruben, J-M. Lehn, P. Müller. *Chem. Soc. Rev*., **35**, 1056 (2006).
[9] Q. Zeng, D. Wu, C. Wang, H. Ma, J. Lu, C. Liu, S. Xu, Y. Li, C. Bai. *Cryst. Growth Des*., **5**, 1889 (2005).
[10] P.V. Bernhardt. *Inorg. Chem*., **38**, 3481 (1999).
[11] B.B. Ivanova, M. Spiteller. *Cryst. Growth Des*., **10**, 2470 (2010).
[12] R. Gup, E. Giziroglu, B. Kirkan. *Dyes Pigm*., **73**, 40 (2007).
[13] D. Thetford, A.P. Chorlton, J. Hardman. *Dyes Pigm*., **59**, 185 (2003).
[14] P.T. Muthiah, M. Hemamalini, G. Bocelli, A. Cantoni. *Struct. Chem*., **18**, 171 (2007).
[15] M.S. Masoud, M.F. Amira, A.M. Ramadan, G.M. El-Ashry. *Spectrochim. Acta, Part A*, **69**, 230 (2008).
[16] V.T. Yilmaz, M.S. Aksoy, O. Sahin. *Inorg. Chim. Acta*, **362**, 3703 (2009).
[17] V.T. Yilmaz, F. Yilmaz, H. Karakaya, O. Büyükgüngör, W.T.A. Harrison. *Polyhedron*, **25**, 2829 (2006).
[18] L.-F. Ma, L.-Y. Wang, Y.-Y. Wang, S.R. Batten, J.-G. Wang. *Inorg. Chem*., **48**, 915 (2009).
[19] Q.-M. Wang, T.C.W. Mak. *Inorg. Chem*., **42**, 1637 (2003).
[20] M.G. Amiri, A. Morsali, A.D. Hunter, M. Zeller. *Solid State Sci*., **9**, 1079 (2007).
[21] A. Aslani, A. Morsali, M. Zeller. *Solid State Sci*., **10**, 854 (2008).
[22] S.H. Kim, B.K. Park, Y.J. Song, S.M. Yu, H.G. Koo, E.Y. Kim, J.I. Poong, J.H. Lee, C. Kim, S-J. Kim, Y. Kim. *Inorg. Chim. Acta*, **362**, 4119 (2009).
[23] U. García-Couceiro, O. Castillo, A. Luque, J.P. García-Terán, G. Beobide, P. Román. *Cryst. Growth Des*., **6**, 1839 (2006).
[24] *CryAlis RED*, *Version 1.171.32.38* (release 17-11-2008 CrysAlis171. NET) (Compiled Nov 17 2008, 13:58:09), Oxford Diffraction Ltd., Abingdon, UK.
[25] G.M. Sheldrick. *SHELXL-97 – A Program for Crystal Structure Refinement*, University of Gottingen, Germany (1997).
[26] A.C. Larson. *Crystallogr. Compounds*, 291 (1970).
[27] R.H. Blessing. *Acta Crystallogr. A*, **51**, 33 (1995).
[28] L.J. Farrugia. *J. Appl. Crystallogr*., **30**, 565 (1997).
[29] C.F. Macrae, P.R. Edgington, P. McCabe, E. Pidcock, G.P. Shields, R. Taylor, M. Towler, J. van de Streek. *J. Appl. Crystallogr*., **39**, 453 (2006).
[30] G.R. Desiraju. *Acc. Chem. Res*., **35**, 565 (2002).
[31] J.L. Atwood, J.W. Steed. *Encyclopedia of Supramolecular Chemistry*, Taylor & Francis, New York (2004).
[32] H.A. Bent. *Chem. Rev*., **68**, 587 (1968).
[33] B.S. Avvaru, C.U. Kim, K.H. Sippel, S.M. Gruner, M. Agbandje-Mckenna, D.N. Silverman, R. Mckenna. *Biochemistry*, **49**, 249 (2010).
[34] H.C. Garcia, R. Diniz, M.I. Yoshida, L.F.C. de Oliveira. *CrystEngComm*, **11**, 881 (2009).
[35] M.S. Aksoy, V.T. Yilmaz, O. Buyukgungor. *J. Coord. Chem*., **62**, 3250 (2009).
[36] V.T. Yilmaz, F. Yilmaz, E. Guney, O. Buyukgungor. *J. Coord. Chem*., **64**, 159 (2011).
[37] R.N. Westhorpe, C. Ball. *International Congress Series*, **1242**, 57 (2002).
[38] V.A. Blatov, IUCr *Compcomm Newsletter*, **7**, 4 (2006). Available online at: http://www.topos.ssu.samara.ru (accessed January 30, 2011).
[39] L.F.C. de Oliveira, P.S. Santos, J.C. Rubim. *J. Raman Spectrosc*., **22**, 485 (1991).
[40] M. Kurt, S. Yurdakul. *J. Mol. Struct*., **654**, 1 (2003).
[41] M. Ristova, G. Petrusevski, A. Raskovska, B. Soptrajanov. *J. Mol. Struct*., **924**, 93 (2009).
[42] A.J. Barnes, L. Legall, J. Lauransan. *J. Mol. Struct*., **56**, 15 (1979).
[43] M.V. Marinho, M.I. Yoshida, K.J. Guedes, K. Krambrock, A.J. Bortoluzzi, M. Hörner, F.C. Machado, W.M. Teles. *Inorg. Chem*., **43**, 1539 (2004).